Engineering Structures 61 (2014) 1–12

Contents lists available at ScienceDirect

Engineering Structures

journal homepage: www.elsevier.com/locate/engstruct

Response of normal-strength and ultra-high-performance fiber-reinforced concrete columns to idealized blast loads

Serdar Astarlioglu *, Ted Krauthammer

Center for Infrastructure Protection and Physical Security, University of Florida, 365 Weil Hall, Gainesville, FL 32611, USA

ARTICLE INFO

Article history:
Received 1 February 2013
Revised 1 January 2014
Accepted 8 January 2014
Available online 2 February 2014

Keywords:
Reinforced concrete
Ultra-high-performance-fiber-reinforced concrete
Columns
SDOF analysis
Blast loads
Load–impulse (P–I) diagrams

ABSTRACT

A numerical study was used to study the response of a normal-strength concrete (NSC) column that was not design for blast resistance subjected to four levels of idealized blast loads. Then, to compare the behavior of the NSC column with a column made with ultra high performance fiber reinforced concrete (UHPFRC) that had the same dimensions and reinforcing details as the NSC column and subjected to the same loading conditions. The boundary conditions and the level of compressive axial load due to gravity were also considered in the analyses. The behavioral comparisons were made both in the time-history domain, as well as in the load–impulse (P–I) domain. Comparisons, observations, and conclusions are presented.

1. Introduction

More than three decades of research on innovative concrete materials such as DUCTAL [1], $\text{CEMTEC}_{\text{multiscale}}$ [2], CeraCem [3], COR-TUF [4], and others have resulted in concrete materials with compressive strengths in excess of 160 MPa. These cementitious composites, with the incorporation of steel fibers in the mix, form a new class of concrete that is termed ultra-high-performance fiber-reinforced concrete (UHPFRC) that offers increased strength, ductility, and durability compared to normal- and high-performance concrete materials. These improved properties in the material level are expected to translate to improved performance and resilience in the overall structural level, even when the structure is subjected to highly impulsive loads such as blast or impact. There have been some recent studies on the response of UHPFRC-based structural beams and slabs under severe dynamic loads [5–11]. However, we have a very limited knowledge base on the behavior of UHPFRC columns under such extreme loads. Considering that columns are essential to the survival of a structure after a blast, and that abrupt failure of such structural components may lead to partial or complete progressive collapse, investigating if using UHPFRC instead of normal strength concrete (NSC) for columns is important. Understanding how much improvement can be achieved by using UHPFRC instead of (NSC) in columns that were not designed for blast loads could lead to more options for enhancing a building's blast protection features.

This study was carried out numerically by investigating the nonlinear response characteristics of NSC and UHPFRC columns under blast loads, assuming that the dimensions, support conditions, and reinforcing details are the same for both types of columns. The investigation quantified the difference in structural performance by comparing the columns' responses in both the time domain and in the load–impulse domain (P–I), as will be explained later, herein. The strength and ductility of a column can be strongly influenced by the level of compressive axial force present on the column and by the boundary conditions. Therefore, the level of axial compressive force from gravity loads and the boundary conditions were also considered as variables, in addition to transverse blast loads from charges at various distances. This study aims to expand the previous work by the authors on the blast response of reinforced concrete (RC) columns [12] to include UHPFRC columns by using a UHPFRC-specific material model and by drawing contrasts between the behavioral differences.

2. Numerical approach

This study was conducted using a single-degree-of-freedom (SDOF)-based approach. Although the use of an SDOF-based approach may seem simplistic compared to using a continuum-based finite element approach, using SDOF-based solutions is common practice in the blast assessment of structural components. The SDOF model was validated using detailed finite element analysis

* Corresponding author. Tel.: +1 352 273 0695.
E-mail addresses: serdara@ufl.edu (S. Astarlioglu), tedk@ufl.edu (T. Krauthammer).

0141-0296/$ - see front matter © 2014 Elsevier Ltd. All rights reserved.
http://dx.doi.org/10.1016/j.engstruct.2014.01.015

and with available experimental data. Once validated, the SDOF approach was later used to obtain the P–I diagrams of the NSC and UHPFRC columns.

The SDOF analyses were conducted using the Dynamic Structural Analysis Suite (DSAS), which is an advanced structural analysis program that couples a nonlinear resistance function obtained using a displacement-controlled finite element solver and structural elements with a fast-running SDOF engine [13–15]. DSAS uses a layered/fiber approach and strain compatibility to obtain the moment–curvature relationship of the section of the beam or column under investigation, and then uses a displacement-controlled finite element solver based on Crisfield's arc-length method [16] with nonlinear beam/column elements to obtain the resistance, equivalent load, and equivalent mass functions. The process used for establishing equivalent SDOF system properties based on the real system properties is described below.

As a result of the SDOF approximation, the load function must be separable into time-dependent and spatial components, as shown in Eq. (1):

$$p^t(x) = \lambda^t \bar{p}(x) \tag{1}$$

where $p^t(x)$ is the load function; λ^t the time-dependent portion of the load function, and $\bar{p}(x)$ is the spatial distribution of the load.

Fig. 1 shows a schematic of the structural component and various parameters for which the equivalent SDOF parameters will be defined. Instead of using elastic, elastic–plastic, and plastic displacement profiles to determine load and mass factors, as suggested by Biggs [17], DSAS uses a displacement-controlled finite element solver to determine the displacement field for each load/displacement increment i. Once the displacement field at load increment i is determined, the shape function for the load stage is determined from Eq. (2) by dividing the entire displacement field by the reference displacement at a preselected location along the span (i.e., midspan) as defined in Eq. (3):

$$\varphi^i(x) = \frac{u^i(x)}{u^i_m} \tag{2}$$

$$u^i_m = u^i\left(\frac{L}{2}\right) \tag{3}$$

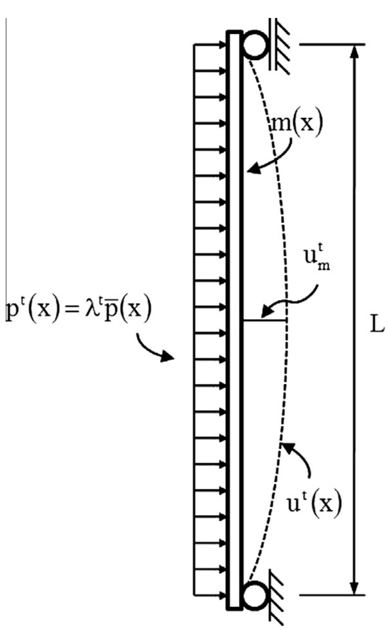

Fig. 1. The real structural member.

in which $u^i(x)$ is the displacement field at load increment i; u^i_m the reference displacement at load increment i (i.e., midspan displacement), and $\varphi^i(x)$ is the normalized shape function at load increment i.

Once the load distribution, shape function, and reference displacement values are obtained corresponding to all the load increments, the equivalent load is determined from Eq. (4), as suggested by Biggs [17]:

$$F^i_e = \int_0^L p^i(x) \cdot \varphi^i(x) \cdot dx \tag{4}$$

in which $p^i(x)$ is the load distribution on the real system at load increment i; F^i_e the equivalent load on the SDOF system at load increment i, and L is the span length of the member.

Eq. (4) ensures that the strain energies of the real and the equivalent SDOF systems are identical. In a similar fashion, by equating the kinetic energies of the real and the equivalent SDOF systems, the equivalent mass function at a given load increment i is determined from:

$$M^i_e = \int_0^L m(x) \cdot [\varphi^i(x)]^2 \cdot dx \tag{5}$$

in which $m(x)$ is the mass distribution on the real system and M^i_e is the equivalent mass of the SDOF system at load increment i.

The determination of equivalent load and mass functions is achieved using nonlinear static analysis. As a consequence, the superscript t, indicating time step in Eq. (1) and Fig. 1, is replaced with i, indicating load/displacement increment step in Eqs. (2)–(5).

Once the static analysis is completed and all of the equivalent SDOF system parameters are determined as a function of the reference displacement, the Newmark-Beta method [18] is used to solve the dynamic equilibrium equation shown below:

$$F^t_e = M^t_e \ddot{u}^t_m + C\dot{u}^t_m + R^t_e \tag{6}$$

in which $R^t_e = R_e(u^t_m)$ is the equivalent resistance at time t, $M^t_e = M_e(u^t_m)$ the equivalent mass at time t, $F^t_e = \frac{F_e(u^t_m)}{\lambda(u^t_m)}\lambda^t$ the equivalent load at time t, $\ddot{u}^t_m, \dot{u}^t_m, u^t_m$ the displacement, velocity, and acceleration at the reference location at time t (i.e., midspan), and C s the damping coefficient.

A P–I diagram is a specialized form of response spectrum that relates the peak load (e.g., peak reflected pressure) and impulse generated by a certain loading scenario to damage level on a specific component. The process for obtaining the P–I diagram numerically is described in detail in Krauthammer et al. [19], where the SDOF analysis engine is used to carry out bisection iterations to find the threshold curve. This approach obviously requires a significant number of SDOF analyses to obtain a single P–I curve for a specific load shape (e.g., a triangular pulse) and is consequently computationally very time intensive. The loading scenario might be a triangular or exponential function to represent idealized blast pressure time-history and the damage level might be a specific displacement, acceleration, support rotation level, or a certain failure mode (e.g., flexure with or without diagonal shear, direct shear, etc.). Although the procedure described above was used to conduct a single time-history analysis, it can also be incorporated into a search algorithm to obtain the P–I threshold curve, as shown in Fig. 2. The search algorithm relies on selecting an origin pressure and impulse combination that corresponds to a specific structural response threshold (I_p, P_p), as shown in Fig. 2(a). Instead of determining the origin point by trial and error, one can use the expressions for impulsive and quasi-static asymptotes [13], shown in Eqs. (7) and (8), respectively, to estimate the location of the asymptotes and then use these values to select an origin point that is located toward the right of the impulsive asymptote and above the quasi-static asymptote.

$$\text{Impulsive domain : Kinetic Energy} = \text{Strain Energy} \tag{7}$$